Research Article

Elution behavior of shortened multiwalled carbon nanotubes in size exclusion chromatography

Wonmok Lee[1]
Young Jin Cho[1]
Heung Ryul Choi[2]
Hye Jin Park[3]
Taihyun Chang[2]
Min Park[3]
Hyunjung Lee[4]*

[1] Department of Chemistry, Sejong University, Gunja-Dong, Gwangjin-Gu, Seoul, Korea
[2] Department of Chemistry and Division of Advanced Materials Science, Pohang University of Science and Technology (POSTECH), Pohang, Korea
[3] Hybrid Materials Center, Korea Institute of Science and Technology, Seongbuk-gu, Seoul, Korea
[4] School of Advanced Materials Engineering, Kookmin University, Jeongneung-Dong, Seoul, Korea

Received May 29, 2012
Revised August 2, 2012
Accepted August 2, 2012

We present a rigorous investigation on elution behaviors of ultrasonically shortened multiwalled carbon nanotubes in size-exclusion chromatography. The size separation of five carbon nanotube samples that underwent ultrasonic shortening for varying lengths of time revealed the existence of three kinds of carbon species: large nanotubes, small nanotubes, and amorphous carbon species. Separation of the three different carbon species was confirmed by SEM analyses on the fractionated eluates and also by light scattering/UV absorbance double detection. The chromatographic peak intensity ratio between the large and small nanotubes suggested an increased amount of small carbon nanotubes upon longer mechanical treatment time. The effect of the concentration of carbon nanotube dispersion on elution behavior was examined, and the elution volume of the shortened nanotubes was found to decrease upon dilution while that of the large nanotubes showed the opposite tendency. Unusual elution behaviors of the multiwalled carbon nanotubes were also observed by altering the flow rate, and these behaviors could be explained by the longer equilibration time taken for large nanotubes to access the pores of the packing materials and a possible morphology change of small carbon nanotubes.

Keywords: Fractionation / Light scattering detection / Multiwalled carbon nanotube / Size-exclusion chromatography / Ultrasonic shortening
DOI 10.1002/jssc.201200489

1 Introduction

Carbon nanotubes (CNTs) are promising materials for various industrial applications by virtue of their superior electrical and mechanical properties [1]. Appropriately purified CNTs can be applied to various electronic and photonic devices. Extensive work has been devoted to the development of effective synthetic routes for single-walled carbon nanotubes (SWCNTs) and multiwalled carbon nanotubes (MWCNTs). In general, as-synthesized CNTs contain amorphous carbon species and catalyst, and they have complex three-dimensional structures and length distributions. Compared to MWCNTs, SWCNTs are simpler from a structural point of view, exhibiting either metallic or semiconducting properties depending on the molecular structure. Their physical properties are further affected by length, diameter, and the distributions of these size parameters. Needless to say, the properties of MWCNTs are even more diverse. Since the purification of CNTs is a critical factor toward actual device applications, a variety of strategies for the separation and characterization of CNTs have been explored. The separation of metallic and semiconducting SWCNTs has been demonstrated by several groups [2–4]. Length sorting is also an important process, as longer and micron-scale CNTs with high aspect ratios are particularly useful in field emission displays and electron conducting films [5–7]. On the other hand, short CNTs can be utilized as electrical conducting wires in molecular devices [8]. The length tuning of CNTs can be done by chemical treatment using strong acid, but this process suffers from poor reproducibility and often results in loss of electrical conductivity by producing defects in the pristine CNTs [8, 9]. Mechanical cutting by ball milling [10–12] or ultrasonication [13, 14] can be utilized instead of or in conjunction with the chemical treatment to obtain length-tuned CNTs. Over the last decade, LC separations of CNTs based on their sizes have been demonstrated using ion-exchange chromatography (IEC) [15, 16], HPLC [17], and size-exclusion chromatography (SEC) [18, 19]. Other separation techniques such as field flow fractionation [20, 21] and capillary electrophoresis [22–24] have also been investigated as size-dependent fractionation tools for CNTs. Zheng et al. successfully carried out the chromatographic separation and length sorting of SWCNTs by wrapping them with

Correspondence: Hyunjung Lee, School of Advanced Materials Engineering, Kookmin University, Jeongneung-Dong, Seoul, Korea
E-mail: hyunjung@kookmin.ac.kr
Fax: +82-2-910-4317

Abbreviations: CNT, carbon nanotube; **LS**, light scattering; **MWCNT**, multiwalled carbon nanotube; **PS**, polystyrene; **SWCNT**, single-walled carbon nanotube

---

*Additional correspondence: Professor Wonmok Lee,
E-mail: wonmoklee@sejong.ac.kr

single-stranded DNA in water [15,16]. They used an anion exchange chromatographic technique to effectively separate the water-soluble SWCNT–DNA assemblies. Zhao et al. reported the SEC separation of SWCNTs functionalized with octadecyl amine to enhance their solubility in organic solvent [19]; they achieved the separation of SWCNTs from large globular impurities and amorphous carbon species. So far, most of the chromatographic methodology developed for the separation of SWCNTs has relied on functionalization using water-soluble molecules. Even though this provides good dispersion in aqueous medium, surface functionalization may deteriorate the CNT's mechanical or electrical properties. The size sorting of MWCNTs has rarely been studied, probably due to the more complex structure of MWCNTs, which makes chromatographic separation less reproducible and hard to interpret. Duesberg and coworkers demonstrated SEC separation of micellar aqueous dispersions of MWCNTs [25]. Recently, we also have reported size separation of the shortened MWCNTs [14], however, the chromatographic resolution was not satisfactory. In this study, we employed two serially connected SEC columns to investigate the high-performance SEC separation of MWCNTs shortened by ultrasonication for varying lengths of time. By controlling various chromatographic conditions such as detectors, concentration, and flow rate, we were able to perform an in-depth investigation of the SEC elution behaviors of MWCNTs.

2 Material and methods

2.1 Sample preparation

A pure MWCNT sample was received as a kind gift from Korea University. This was synthesized by chemical vapor deposition (CVD) in acetylene gas using Fe-Mo/Al_2O_3 as the catalyst [26,27]. As characterized in our previous study, the average diameter of the MWCNTs was 10–30 nm, and the sample contained less than 5% mixed impurities of catalyst and amorphous carbon species [14]. More details of the MWCNTs used in this study can be found in our previous reports [14,26,27]. In this study, MWCNT samples underwent length tuning by chemical and ultrasonic treatment using five different sets of conditions schematically illustrated in Fig. 1. To enhance their compatibility with polar solvents, MWCNTs were first treated with a solution of concentrated H_2SO_4 (98%)/HNO_3 (70%) (3:1 v/v) at ambient temperature for 4 h. After rinsing with deionized (DI) water to remove residual acids, the CNTs were freeze-dried overnight. MWCNT samples were then dissolved in DMF to a 1 mg/mL concentration, and ultrasonic etching was carried out for 3, 4, 5, 6, and 9 h using a high power ultrasonic system (330 W, Hielscher Ultrasonics). Two-second ultrasonic pulses were applied to the samples in 5-s intervals. The resulting MWCNT samples were denoted using the convention A*n*S*m*, where *n* and *m* describe the acid treatment and sonication time, respectively. In this study, we investigated only the effect of ultrasonic cutting on MWCNTs for different sonication times under a fixed acid treatment time of 4 h. High-power ultrasonication has been confirmed as a useful method for shortening MWCNTs with a narrow length distribution.

2.2 Chromatographic analysis

The pretreated MWCNT samples remained well dispersed in DMF for several days without sedimentation or flocculation. Nonetheless, the samples were again dispersed using a bath sonicator for 1 h, and centrifuged at 13 000 rpm using an ultracentrifuge system (Gyrogen Gyrospin A-32010) prior to SEC separation. After centrifugation for 30 min, an upper phase comprising a gray dispersion was formed, which was easily distinguishable from the bottom sediment. Since the sedimented CNTs were too large for chromatographic separation, the upper phase was used in most of our investigations. Some MWCNT samples were diluted prior to separation in order to explore the concentration effect.

The SEC system used in this study consisted of a dual head gradient pump (Acme-9000 series, Young Lin), 6-port Rheodyne injector, and a UV-Vis absorbance detector operated at 300 nm (the maximum absorbing wavelength of our MWCNTs). Two large pore-size SEC columns (PL-gel Mixed-A, Polymer Laboratory) were serially connected for the separation of the large MWCNTs with an inline filter (pore size 10 μm, sweep volume 20 μL) placed between the injection loop and the columns to prevent clogging of the aggregated CNTs or other particulates at the column inlet.

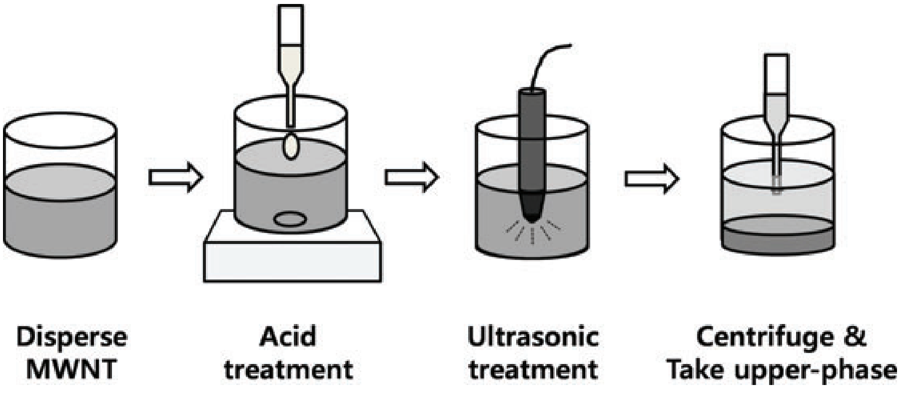

Figure 1. Experimental procedure for MWCNT sample preparation.

For direct analysis of the size of the eluting MWCNTs, a multiangle light scattering (MALLS, Wyatt, mini-DAWN) detector was connected before the UV detector (see Supporting Information Fig. S1 in the supporting data S1 for the instrumentation employed in this study). The injection loop size was 100 μL, and the flow rate of DMF was typically 0.8 mL/min but was lowered down to 0.1 mL/min to examine the flow rate dependence. In order to indicate the estimated size of MWCNTs at each elution time, the calibration curve was obtained using five polystyrene (PS) standards with various molar masses. They were separately injected under the same chromatographic condition for MWCNT analysis and their radius of gyrations (R_g) was cited from the previous literatures [28]. To observe the eluted MWCNTs directly, the eluates were collected on an alumina filter frit (pore size 0.02 μm, Anodisc13, Whatman) through which the DMF solvent was removed by aspiration. Upon removal of the majority of the DMF, the fractionated MWCNTs on the alumina frit were dried in a vacuum oven at 80°C overnight, and SEM (HITACHI, S-4700) analysis was carried out. In situ elemental analysis of MWCNTs and amorphous carbon species was performed using energy dispersive X-ray (EDX, HORIBA 7200-H) spectroscopy in conjunction with SEM.

3 Results and discussion

In order to characterize the chromatographically fractionated MWCNTs and amorphous carbon species, SEC eluates were collected during the elution of the three representative peaks shown in Fig. 2. For fractionation, the original dispersion of the uncentrifuged A4S9 was used, and drops of eluate from the three fractions were directly transferred onto three separate porous alumina filters under aspiration for ~1 min; the liquid eluent was drained, leaving the carbonaceous species on top of the filters. The dried fractions were characterized by SEM. As shown in Fig. 2, Fraction 1 collected at $t_R = 9$–11 min consisted mostly of large MWCNTs. The elution time of 10 min corresponds to the total exclusion limit of the columns within which any molecules larger than the maximum pore size of the SEC packing material are eluted through the interstitial spaces without accessing the pores. Therefore, the peak observed for 9–11 min elution was expected to correspond to MWCNTs too large to be separated by the SEC columns used in this study. SEM images of Fraction 2, however, revealed the presence of short MWCNTs. The length distributions were obtained from SEM images of Fractions 1 and 2, (see Supporting Information Fig. S2) and the number-averaged lengths were calculated to be 128 and 75 nm, respectively.

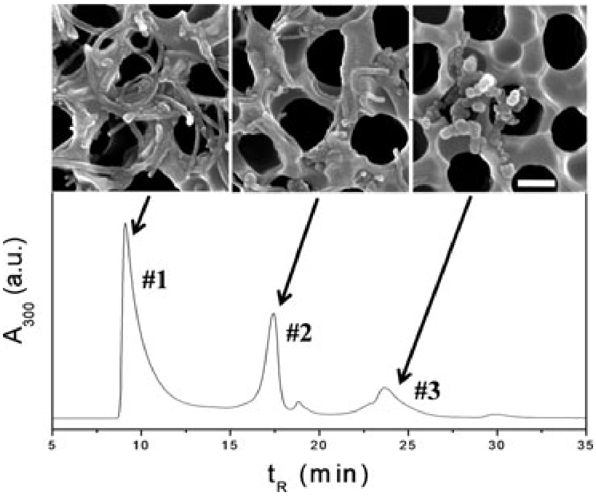

Figure 2. SEC separation and fractionation of uncentrifuged-A4S9 samples at three different elution times. SEM images of each fraction on porous alumina filter are also shown. Fraction 1 mostly contained long MWCNTs while Fraction 2 contained small fragmented CNTs. Far less material was captured on the alumina filter from Fraction 3. The magnification of the three SEM images is the same; the scale bar in the SEM image corresponding to Fraction 1 is 200 nm.

The SEM image of Fraction 3 (Fig. 2) revealed a non-tubular, presumably amorphous, carbon species. EDX elemental analyses were performed on the MWCNTs and amorphous carbon species in conjunction with the SEM imaging to confirm their chemical identities. Although not shown here, long MWCNTs were occasionally found in Fractions 2 and 3, which could be attributed to slow mass transfer of the large CNTs. Unable to quickly follow the size-exclusion equilibrium, some of the MWCNTs might either get trapped within the pores and then randomly elute during the chromatographic run, or even pass through the interstitial spaces without accessing the pores of the packing material. In addition to the slow mass transfer rates, a strong attractive force existing between the CNTs and packing material may explain the poor size separation efficiency. It is well known that chromatographic elution of an adsorptive species often causes peak tailing or poor mass recovery.

Figure 3 shows the SEC chromatograms of the five MWCNT samples after centrifugation at 13 000 rpm for 10 min to remove the large CNTs. The chromatograms are shown in the order of increasing sonication time, i.e. 3–9 h from A4S3 to A4S9. Along with the chromatograms, a calibration curve (R_g versus t_R) obtained from PS narrow standards is also shown in Fig. 3 to indicate the estimated size of the MWCNTs at each elution time. In proper solvent, the radius of PS and its average molar mass satisfy the following relationship [28]:

$$R_g\,(\text{nm}) \approx 0.0118 \times M_w^{0.6}\ (\text{PS in tetrahydrofuran at } 25^\circ\,\text{C}) \tag{1}$$

The calibration curve in Fig. 3 was obtained based on Eq. (1) using the molar mass of five PS species. According to this curve, the R_g of the PS eluted at 17 min (the elution time of the second peak of A4S3) was calculated to be 47 nm, which roughly coincides with the mean size of the shortened MWCNTs (75 nm) observed in the SEM image shown in Fig. 2. In each chromatogram of Fig. 3, the first eluting peak is observed at 9–11 min. These peaks correspond to the MWCNTs that were too large to be separated by the SEC columns.

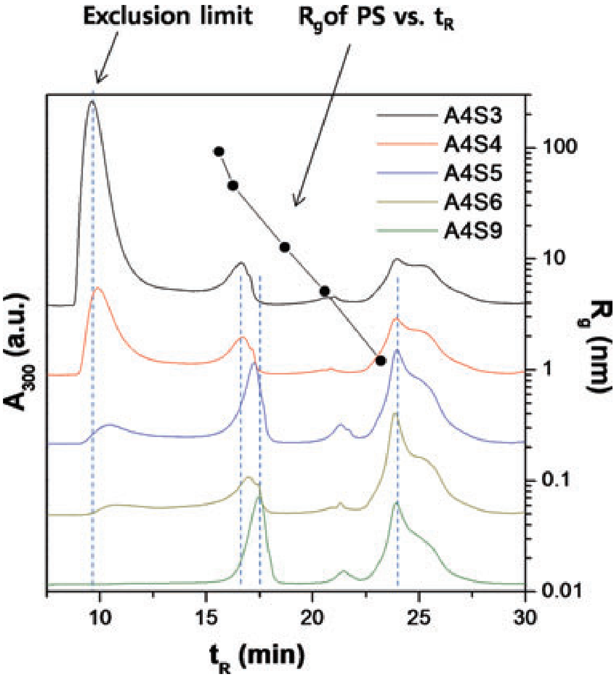

Figure 3. SEC chromatograms of the five different MWCNT samples after removal of aggregated CNTs by centrifugation. UV detection clearly indicated a consistent decrease in first peak area for large MWCNTs (~10 min) at longer sonication times and an increase in shortened MWCNT peaks (17–17.5 min). Peaks at ~24 min are due to amorphous carbon species. SEC calibration curve of PS standards in DMF is also plotted to demonstrate elution time of macromolecules in the SEC columns.

Zhao et al. used the same type of SEC column for SWCNT separation. The earliest elution peak of SWCNTs they observed was at the same elution volume as ours [19]. However, in contrast to the chromatogram in Fig. 2 (before centrifugation), the first peak in the A4S9 chromatogram at ~9 min completely disappeared. From Fig. 3, it is obvious that longer sonication times of the MWCNTs resulted in lower amounts of long CNTs, showing the effective shortening. Following the peak at 9–11 min, the second characteristic peak appeared at about 17–17.5 min for each sample, corresponding to the shortened MWCNTs. It is readily apparent that the peak intensity ratios of the second peak increased with increasing sonication time as compared to the first peak. The changes in peak intensities arises from the increased ratio of shortened MWCNTs to long ones with longer sonication times due to the effective ultrasonic cutting of CNTs. The reproducibility of the elution behavior was confirmed by independent SEC runs of each sample on different days and by injecting them in random sequences. A closer look at Fig. 3 reveals that in addition to the relative peak intensities, the retention time of the second peak also changed with increasing sonication time, becoming a little longer. For instance, the retention time of shortened CNTs for A4S3 was 16 min while that for A4S9 was 17 min. This indicates that longer sonication treatment further shortens the lengths of the MWCNTs. After elution of the two characteristic MWCNT peaks at ~10 and 17 min, small peaks appeared at around 22 min followed by large overlapping peaks eluting at ~24 min. The small peaks at around 22 min are shortened MWCNTs. A significant light scattering (LS) signal in Fig. 4 confirms that these peaks are not small-sized amorphous carbons. The peaks at 24 min appear to be fragmented amorphous carbon species rather than MWCNTs, especially considering that the elution time of 24 min corresponds to the molecular weight of PS of <1000, which is very small in terms of hydrodynamic size. Overall, the chromatograms in Fig. 3 demonstrated improved resolution of SEC separation compared to previous investigations, presumably due to the use of two SEC columns and the inline filter as well as the removal of extremely large CNTs by ultracentrifugation [14].

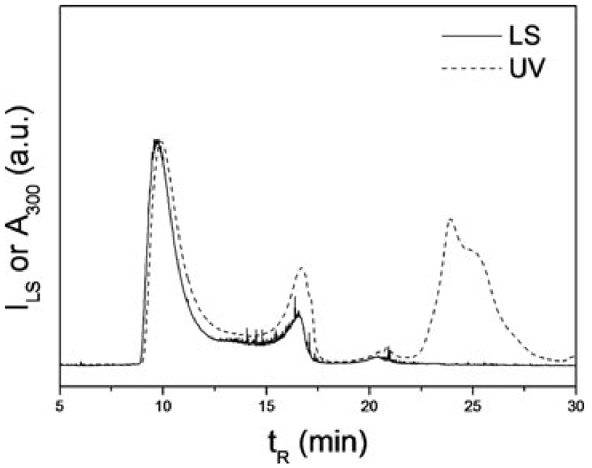

Figure 4. UV-LS double detection of A4S4 during SEC separation. The two detector responses are overlaid, and the intensities of the two signals are normalized to the earliest eluting peaks.

SEM images of the fractionated MWCNTs in Fig. 2 allowed a direct visualization of individual CNTs with different lengths, but these may not be representative of the eluting species as some of nanotubes were able to pass though the alumina filter. To obtain size information for the eluting peaks in more inclusive way, mass-sensitive LS detection was used in conjunction with a concentration-sensitive UV-Vis detector. LS signal intensity is proportional to the differential index of refraction (d*n*/d*c*) in a given eluent as well as the absolute molecular weight of the macromolecule. We confirmed that the refractive index (RI) detector, another concentration-sensitive detector, produced very similar chromatograms to those produced by UV detection for our MWCNT samples (see Supporting Information Fig. S3). Thus, the use of UV as a concentration detector for LS analysis was deemed reasonable. Nonetheless, only a relative comparison of LS and concentration detection was made for the representative peaks since quantitative size analysis was impossible due to strong light absorption and complex architectures (i.e. tube diameter, number of layers, etc.) of the MWCNTs hampering Rayleigh LS.

In Fig. 4, LS and UV chromatograms obtained from A4S4 were plotted with the intensities of both signals normalized

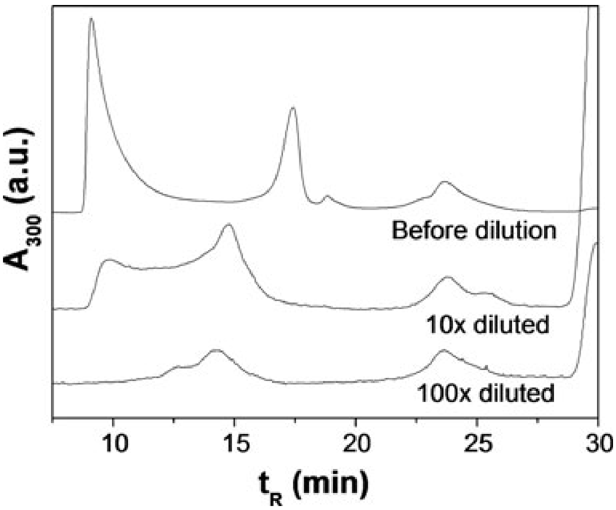

Figure 5. Concentration effect on SEC elution of A4S9 MWCNT sample: from the top, uncentrifuged A4S9 stock solution, ten-fold diluted sample, and 100-fold diluted sample, respectively.

to the earliest eluting peaks. At first glance, very strong LS signals from CNT species despite low concentrations (<0.1 mg/mL) indicated that they extensively scattered the incident light, presumably due to their large size. It is reasonable that the early eluting peak at ∼10 min contained smaller MWCNTs than those in the second peak at ∼17 min, since the second peak produced lower LS signals than UV signals compared to the first eluting peak. Interestingly, amorphous carbon species did not produce any LS signal, clearly demonstrating that they were very small in size. To simplify the interpretation of the double detection signals, the d*n*/d*c* of the eluting species were assumed to be the same, which might not be a sound assumption. We obtained LS/UV double detection chromatograms for full sets of MWCNTs, which are shown in Supporting Information Fig. S4. The comparison of the relative intensity ratio of the shortened and large MWCNTs with respect to the ultrasonication time was, however, not straightforward due to the complexity of MWCNT structures as discussed above.

To investigate the effect of sample concentration on elution, the original A4S9 sample in DMF with an initial concentration of ∼1 mg/mL was diluted ten- and 100-fold using the eluent. The resulting SEC chromatograms are compared in Fig. 5. In order to compare dilution effects on the elution of CNTs of different lengths, the uncentrifuged A4S9 sample was used. Since the detected peak intensities were decreased by dilution, the intensity scales of the chromatograms were enlarged. As shown in Fig. 5, the dilution definitely caused a peak shift of shortened MWCNTs from 17.5 min (before dilution) to 14.9 and 14 min (as indicated by dotted lines in Fig. 5) upon ten- and 100-fold dilution, respectively. The extent of the peak shift was diminished for the more highly diluted sample, and thus the elution time showed an asymptotic behavior. The relative peak intensity of the exclusion limit was decreased by dilution and shifted somewhat to a higher elution time. Consequently, the exclusion limit peak completely disappeared, leaving behind a relatively small shoulder-like peak at ∼12.5 min for the 100-fold diluted sample. To show the dilution effect in a different way, fractionation of the separated peaks of an ultracentrifuged A4S9 sample and the fractionated aliquots were reinjected. The experimental details are shown in the supporting data S5, from which we reached the same conclusion as that made for the elution behavior of the diluted samples (see Supporting Information Fig. S5 for detail). As discussed above, the peak shift caused by dilution can be regarded as a unique phenomenon for SEC elution of MWCNTs. The invariant elution time of the amorphous carbon species before and after fractionation is also consistent with the absence of the dilution effect in Fig. 5.

What then would be the origin of the abnormal elution behavior of MWCNTs upon dilution? The complex elution behavior of the MWCNTs can be considered from two different viewpoints: (1) dynamics and (2) equilibrium behavior during SEC separation. The elution behavior of the large, intact MWCNTs should be considered from a dynamics point of view. Certainly, extremely large CNTs cannot be separated by SEC due to their total exclusion from the packing material. Moderately sized MWCNTs are likely to be challenging to separate by SEC since they have larger hydrodynamic volumes than the polymer chains with similar contour lengths due to their rod-like structure, making the diffusivity slower. During chromatographic separation, large molecules are subject to a quasi-equilibrium state in the size-exclusion process as they move through the column and may have insufficient time for pore access under high flow rates [29]. This assumption is supported by the elution behavior at different flow rates, as shown in Fig. 6. In this figure, the chromatograms were drawn with respect to the retention volume (V_R) instead of the retention time (t_R) to better compare the eluted peak positions at different flow rates.

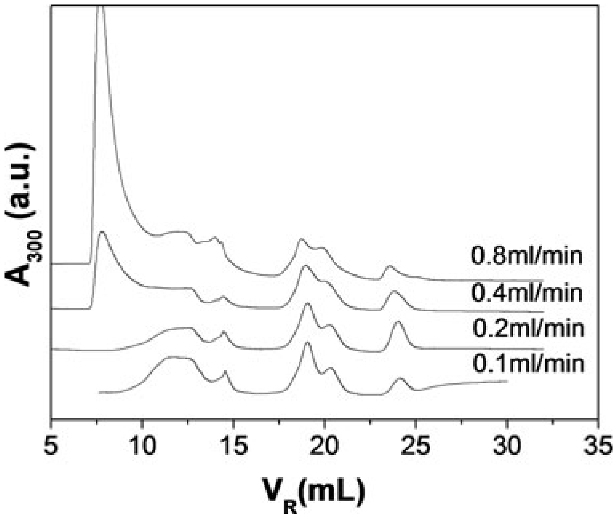

Figure 6. Flow rate effect on SEC elution of MWCNTs (sample A4S4). For better comparison, each chromatogram was plotted versus retention volume (V_R; $t_R \cdot$ flow rate).

If the access of large MWCNTs to the pores was hampered due to slow diffusion, we anticipate that lowering the flow rate would both diminish the experimental artifacts and improve the chromatographic resolution. As shown in Fig. 6, the most noteworthy difference caused by lower flow rates was the decreased intensity of the peak at the exclusion limit, which completely disappeared when the flow rate was lower than 0.2 mL/min; further lowering of flow rate did not affect the chromatogram. At the same time, low flow rates corresponded to an increase in the intensity of a broad peak eluting at 10–13 mL. Experimental results suggested that the equilibrium elution volumes of large CNTs were expected around 10–13 mL, indicating a broad size distribution of the MWCNTs. The other peaks resulting from the shortened MWCNTs ($V_R \sim 14.5$ mL) and the amorphous carbon species ($V_R \sim 19$ mL) did not noticeably change at different flow rates, although the separation resolution of two peaks at 19.5 and 20.5 mL clearly improved at lower flow rates; this is likely due to the fact that CNTs had sufficient time to access pores within the column packing material under these conditions. Thus, the elution behaviors of large and shortened CNTs exhibited different responses. Upon dilution, the probability of MWCNT aggregation decreases. The chromatograms of diluted samples in Fig. 5 support this explanation. On the other hand, shortened MWCNTs appear to have been affected by a totally different mechanism. As shown in Fig. 5, short MWCNTs exhibited delayed elution behavior upon dilution, which is opposite to that of large CNTs. Although not clearly understood at present, it is possible that the short MWCNTs had different molecular anisotropy at different concentrations. At relatively high concentrations, short MWCNTs took on a twisted shape, leading decreased length efficiency. When diluted, their length efficiency improved (i.e. stretching of CNT) and actually increased their hydrodynamic volume [30]. More rigorous investigations are necessary from experimental as well as theoretical standpoints to elucidate the concentration-dependent chromatographic behavior of short MWCNTs more precisely.

4 Concluding remarks

The SEC elution behaviors of the shortened MWCNTs were rigorously examined. By using two mixed bed columns, high-resolution separation of large CNTs, shortened CNTs, and amorphous carbon species was achieved. Centrifugation of MWCNT samples enabled better visualization of size-separated peaks by removing long CNTs that were too large to be separated by SEC. While the elution behavior of amorphous carbon species was insensitive to variations in chromatographic conditions such as sample concentration and flow rate, that of the MWCNTs exhibited a strong dependence on the conditions, particularly the elution time. It was noteworthy that the elution time (or volume) of the large MWCNTs was increased both by diluting the injected sample and by decreasing the flow rate, while the shortened MWCNTs exhibited a decreased elution time after dilution.

W. L. and T. C. acknowledge the support by the Center for Electro-Photo Behaviors in Advanced Molecular Systems at POSTECH (No. 2012-0000532).

H. L. acknowledges the support by Basic Science Research Program through the NRF funded by the MEST(NRF-2011-0014376) and partly by the 2012 research program of Kookmin University in the Republic of Korea.

The authors have declared no conflict of interest.

5 References

[1] Iijima, S., *Nature* 1991, *354*, 56–58.

[2] Arnold, M. S., Green, A. A., Hulvat, J. F., Stupp, S. I., Hersam, M. C., *Nat. Nanotechnol.* 2006, *1*, 60–65.

[3] Maeda, Y., Kimura, S.-i., Kanda, M., Hirashima, Y., Hasegawa, T., Wakahara, T., Lian, Y., Nakahodo, T., Tsuchiya, T., Akasaka, T., Lu, J., Zhang, X., Yu, Y., Nagase, S., Kazaoui, S., Minami, N., Shimizu, T., Tokumoto, H., Saito, R., *J. Am. Chem. Soc.* 2005, *127*, 10287–10290.

[4] Chen, Z., Du, X., Du, M.-H., Rancken, C. D., Cheng, H.-P., Rinzler, A. G., *Nano Lett.* 2003, *3*, 1245–1249.

[5] Lisunova, M. O., Mamunya, Y. P., Lebovka, N. I., Melezhyk, A. V., *Eur. Polym. J.* 2007, *43*, 949–958.

[6] Lee, J., Jeong, T., Heo, J., Park, S.-H., Lee, D., Park, J.-B., Han, H., Kwon, Y., Kovalev, I., Yoon, S. M., Choi, J.-Y., Jin, Y., Kim, J. M., An, K. H., Lee, Y. H., Yu, S., *Carbon* 2006, *44*, 2984–2989.

[7] Bai, J. B., Allaoui, A., *Compos. Part A* 2003, *34*, 689–694.

[8] Li, J. Y., Zhang, Y. F., *Appl. Surf. Sci.* 2006, *252*, 2944–2948.

[9] Tagmatarchis, N., Zattoni, A., Reschiglian, P., Prato, M., *Carbon* 2005, *43*, 1984–1989.

[10] Chen, L., Pang, X.-j., Zhang, Q.-t., Yu, Z.-l., *Mater. Lett.* 2006, *60*, 241–244.

[11] Kukovecz, A., Kany, T., Konya, Z., Kiricsi, I., *Carbon* 2005, *43*, 994–1000.

[12] Konya, Z., Vesselenyi, I., Niesz, K., Kukovecz, A., Demortier, A., Fonseca, A., Delhalle, J., Mekhalif, Z., Nagy, J. B., Ko, A. A., Osvyh, Z., Kocsonya, A., Bir, L. P., Kiricsi, I., *Chem. Phys. Lett.* 2002, *360*, 429–435.

[13] Jeong, S.-H., Lee, O.-J., Lee, K.-H., Oh, S. H., Park, C.-G., *Chem. Mater.* 2002, *14*, 1859–1862.

[14] Park, H. J., Park, M., Chang, J. Y., Lee, H., *Nanotechnology* 2008, *19*, 335702–335709.

[15] Huang, X., Mclean, R. S., Zheng, M., *Anal. Chem.* 2005, *77*, 6225–6228.

[16] Zheng, M., Jagota, A., Semke, E. D., Diner, B. A., McLean, R. S., Lustig, S. R., Richardson, R. E., Tassi, N. G., *Nat. Mater.* 2003, *2*, 338–342.

[17] Farkas, E., Elizabeth Anderson, M., Chen, Z., Rinzler, A. G., *Chem. Phys. Lett.* 2002, *363*, 111–116.

[18] Chattopadhyay, D., Lastella, S., Kim, S., Papadimitrakopoulos, F., *J. Am. Chem. Soc.* 2002, *124*, 728–729.

[19] Zhao, B., Hu, H., Niyogi, S., Itkis, M. E., Hamon, M. A., Bhowmik, P., Meier, M. S., Haddon, R. C., *J. Am. Chem. Soc.* 2001, *123*, 11673–11677.

[20] Chen, B., Selegue, J. P., *Anal. Chem.* 2002, *74*, 4774–4780.

[21] Peng, H., Alvarez, N. T., Kittrell, C., Hauge, R. H., Schmidt, H. K., *J. Am. Chem. Soc.* 2006, *128*, 8396–8397.

[22] Doorn, S. K., Strano, M. S., O'Connell, M. J., Haroz, E. H., Rialon, K. L., Hauge, R. H., Smalley, R. E., *J. Phys. Chem. B* 2003, *107*, 6063–6069.

[23] Suarez, B., Simonet, B. M., Cardenas, S., Valcarcel, M., *J. Chromatogr. A* 2006, *1128*, 282–289.

[24] Lopez-Pastor, M., Dominguez-Vidal, A., Ayora-Canada, M. J., Simonet, B. M., Lendl, B., Valcarcel, M., *Anal. Chem.* 2008, *80*, 2672–2679.

[25] Duesberg, G. S., Burghard, M., Muster, J., Philipp, G., Roth, S., *Chem. Commun.* 1998, *3*, 435.

[26] Yoon, S. W., Kim, S. Y., Park, J., Park, C. J., Lee, C. J., *J. Phys. Chem. B* 2005, *109*, 20403–20406.

[27] Ha, B., Park, J., Kim, S. Y., Lee, C. J., *J. Phys. Chem. B* 2006, *110*, 23742–23749.

[28] Terao, K., Mays, J. W., *Eur. Polym. J.* 2004, *40*, 1623–1627.

[29] Doi, M. E., Edwards, S. F., *The Theory of Polymer Dynamics*, Oxford University Press, Oxford 1998.

[30] Song, P. C., Liu, C. H., Fan, S. S., *Appl. Phys. Lett.* 2006, *88*, 153111.